Acta Acustica 2025, **9**, 51

https://doi.org/10.1051/aacus/2025037

Available online at:
https://acta-acustica.edpsciences.org

TECHNICAL & APPLIED ARTICLE OPEN ACCESS

Group delay-driven crossover optimization for subwoofer satellite systems at listening position

Jooyoung Kim*

Department of New Media Music, Sangmyung University, Seoul, South Korea

Received 22 April 2025, Accepted 15 July 2025

Abstract – This study explores the influence of crossover frequency on frequency response (FR) irregularities in 2.1-channel subwoofer-satellite systems at listening positions, introducing a data-driven optimization approach that focuses on minimizing the maximum absolute group delay (max |GD|) in low frequency range. While subwoofers paired with satellite speakers are increasingly employed for low-frequency reproduction, the role of phase-related effects, such as group delay (GD), in contributing to FR inconsistencies like amplitude dips has received limited attention in prior research. Experiments were carried out in two different rooms, with FR and GD analyzed over a crossover frequency range of 40–140 Hz. The findings suggest that minimizing max |GD| could reduce FR irregularities, with results from a Fixed Effects model indicating a statistically significant positive relationship between max |GD| and $\Delta_{\text{GD-SPL}}$ (coefficient: 22.274, p-value < 0.0001). An optimization algorithm is proposed to identify a crossover frequency that minimizes max |GD|, offering a phase-focused approach that may enhance low-frequency reproduction for practical applications like studio monitoring and home audio.

Keywords. Crossover frequency, Group delay, Subwoofer, Satellite speakers, Frequency response

1 Introduction

The significance of low-frequency reproduction in audio systems has increased, as evidenced by Oehler et al. [1]. Early studio monitors, such as Yamaha's NS-10 m (discontinued in 2001), exhibited limited low-end response [2]. Today, 2.1-channel stereo systems, comprising two satellite speakers and a subwoofer, are widely used in studios for low-frequency reproduction. A key parameter in these systems is the crossover frequency (ω_c), which separates low frequencies handled by the subwoofer from higher frequencies assigned to the satellites. A suboptimally selected ω_c may cause phase misalignment between the subwoofer and satellites, leading to group delay (GD). This GD can contribute to the frequency response (FR) through interference, such as phase cancellations at overlapping frequencies, resulting in amplitude dips.

To address these challenges, previous studies have explored crossover frequency optimization. Zacharov et al. evaluated subwoofer placement at Bang & Olufsen, finding 85 Hz sufficient for a single subwoofer at room boundaries [3]. Kelloniemi et al. noted that subwoofer positions became detectable above 120 Hz, with no clear dependence on listening angle near 30 degrees [4]. Bharitkar et al. [5] developed an algorithm to minimize spectral deviation in FR, quantified as:

$$\sigma_H(\omega_c) = \sqrt{\frac{1}{P}\sum_{i=0}^{P-1}\left(10\log_{10}|H(\omega_i)| - \Delta\right)^2} \quad (1)$$

where ω_c denotes the crossover frequency, $\sigma_H(\omega_c)$ represents the spectral deviation, P is the number of frequency points, Δ is the mean magnitude $\frac{1}{P}\sum_{i=0}^{P-1} 10\log_{10}|H(\omega_i)|$, and $|H(\omega_i)|$ is the FR magnitude at ω_i. In their study, this approach achieved optimal results at 120 Hz by prioritizing FR flatness, yet it neglects phase effects, potentially overlooking narrow amplitude dips and volume imbalances, as discussed in Section 5.

Other work has explored subwoofer placement and quantity. Miller Synergy Core dismissed LFE below 40 Hz, advocating dual subwoofers in the 45–90 Hz range to mitigate room mode resonances [6]. Martens similarly noted improved spatial imaging with two subwoofers, contingent on low-frequency correlation [7].

In contrast to these methods, which often depend on subjective tuning or magnitude-focused metrics, this study proposes a data-driven approach to optimize ω_c by

*Corresponding author: joe45294529@gmail.com

minimizing the maximum absolute GD ($\max|\mathrm{GD}|$) over a defined frequency range. Excessive GD, caused by rapid phase shifts, misaligns signals and generates FR irregularities. This method tackles non-minimum-phase behavior prevalent in real rooms, addressing limitations of spectral deviation techniques, such as their insensitivity to narrow dips, as elaborated in Section 2.2.

2 Background

2.1 Filter and crossover frequency

In a subwoofer-satellite system, a crossover divides the signal into two paths: one passes through a low-pass filter to the subwoofer, while the other reaches the satellite speakers, which may apply high-pass filtering depending on the system design.

The Butterworth filter, a basic design, reduces amplitude by approximately 3 dB at the cutoff frequency [8]. Its slope increases by 6 dB/octave per order (or pole). Two identical Butterworth filters in series form a Linkwitz–Riley filter: two 1st-order filters create a 2nd-order Linkwitz–Riley filter, and two 2nd-order filters form a 4th-order version [9].

This study employs 4th-order Linkwitz–Riley filters for both subwoofer and satellite speakers. Unlike Butterworth filters, which produce a 3 dB gain at the crossover frequency when low-pass and high-pass cutoffs align, Linkwitz–Riley filters ensure unity gain summation for a flat FR. Their 4th-order design, featuring a 24 dB/octave roll-off, enhances frequency band separation and reduces overlap compared to lower-order options. Higher-order filters, such as 8th-order Linkwitz–Riley (48 dB/octave), were avoided due to increased phase distortion from additional stages, which could introduce excessive GD.

2.2 Phase and group delay

Phase describes a wave's angular position within one cycle, ranging from 0 to 2π (360°) per cycle, with shifts of integer multiples of 2π considered equivalent. This concept is fundamental in audio systems, which are typically assumed to be linear time-invariant (LTI), maintaining a consistent input-output relationship over time.

GD, denoted $\tau_g(\omega) = -\frac{\mathrm{d}\phi(\omega)}{\mathrm{d}\omega}$, measures the rate of phase change with frequency, unlike phase delay $\tau_\phi(\omega) = -\frac{\phi(\omega)}{\omega}$, which tracks absolute time shift [10]. In subwoofer-satellite systems, rapid phase shifts increase GD, introducing excessive GD and causing interference that can appear as FR irregularities in typical listening environments.

Room modes, caused by standing waves in enclosed spaces, often induce sharp phase transitions at modal frequencies. Although room modes are fundamentally modeled as second-order resonant systems, their group delay behavior near resonance is frequently approximated using Lorentzian-like expressions. For instance, a simplified resonant system can be represented by the first-order transfer function:

$$H(j\omega) = \frac{\gamma}{j(\omega - \omega_n) + \gamma}, \tag{2}$$

where ω_n is the modal frequency determined by room geometry, γ is a damping factor associated with energy dissipation, and ω is the angular frequency. This transfer function exhibits a phase response of:

$$\phi(\omega) = \tan^{-1}\left(\frac{-(\omega - \omega_n)}{\gamma}\right), \tag{3}$$

which, upon differentiation, yields a group delay of:

$$\tau_g(\omega) = \frac{\gamma}{(\omega - \omega_n)^2 + \gamma^2}. \tag{4}$$

This classical result captures the peak GD at $\omega = \omega_n$, reflecting the characteristic phase shift caused by a resonant mode. Note that the expression in equation (4) is provided for conceptual illustration only and was not used as a fitting or approximation model in the analysis.

In this study, GD was extracted from measured phase responses using Room EQ Wizard (REW). REW calculates GD numerically from the derivative of the unwrapped phase response, based on logarithmic sine sweeps and FFT-based spectral analysis. This helps visualize and interpret GD features that may be influenced by room modes, reflections, or phase shifts introduced by crossover filters.

This study focuses on minimizing the maximum absolute GD, $\max|\mathrm{GD}| = \max_{\omega_i}\left|-\frac{\mathrm{d}\phi(\omega_i)}{\mathrm{d}\omega}\right|$, across a crossover frequency range of 40–140 Hz (as detailed in Sect. 3.4, or 40–120 Hz in Sect. 5). By reducing $\max|\mathrm{GD}|$, this approach mitigates not only phase distortions but also the combined effects of room modes, multiple modal interactions, reflections, non-minimum-phase behavior prevalent in real rooms, and phase distortions near the crossover frequency caused by the filters applied to subwoofer and satellite speakers. Unlike magnitude-based methods, such as Bharitkar et al.'s spectral deviation minimization (Eq. (1)) [5], which prioritize FR flatness and may overlook phase effects, GD minimization directly addresses these critical phase-related distortions.

2.2.1 Room EQ Wizard (REW)

Room EQ Wizard (REW) is a free software tool designed for acoustic measurement and analysis, widely used in research and professional audio applications. It provides functionalities including FR, impulse response, reverberation time (T_{30}, T_{60}), GD, and distortion analysis. Its sine sweep-based approach, using logarithmic sine sweeps as excitation signals, enables precise analysis of acoustic characteristics. The REW Application Programming Interface (API) supports automated measurement and data extraction, integrating seamlessly into signal processing workflows.

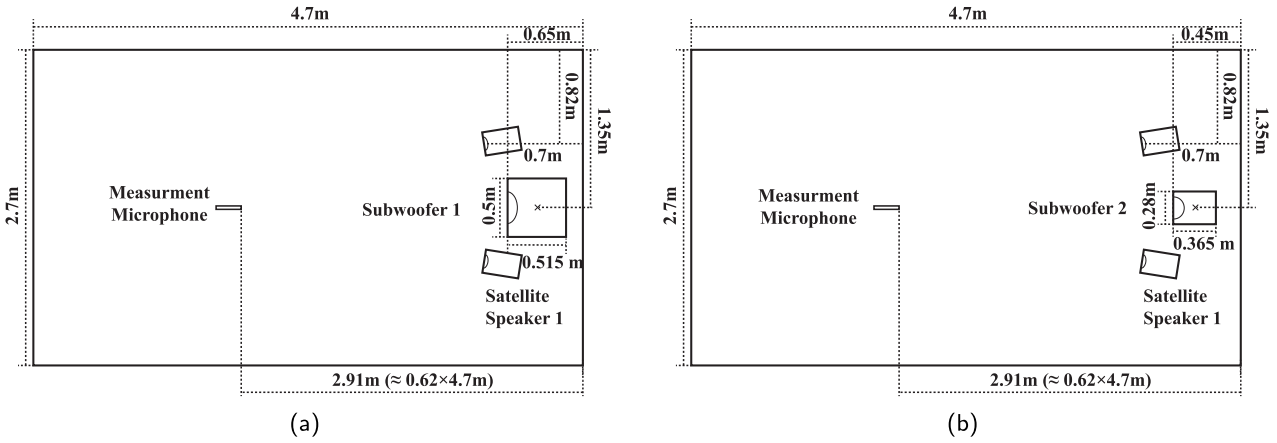

Figure 1. Measurement setups in Room 1 (length × width). (a) Subwoofer 1 and Satellite Speaker Pair 1. (b) Subwoofer 2 and Satellite Speaker Pair 1.

In this study, V5.40 beta 76 was employed to measure FR and GD, analyzing magnitude and phase responses. Measurements utilized a logarithmic sine sweep with a length of 256k samples, corresponding to a sweep duration of approximately 5.46 s at a sampling rate of 48 kHz. The impulse response was analyzed in the frequency domain using REW's Fast Fourier Transform (FFT) processing, with a frequency step of approximately 0.37 Hz, corresponding to an FFT size of 131 072 points. The raw data spanned 0.37 Hz to 20 kHz, with specific bands selected for analysis. All measurements were conducted at a 48 kHz sampling rate, ensuring sufficient resolution for accurate FR estimation. Detailed equipment specifications and analyzed frequency bands are provided in Section 3.

2.2.2 LiveProfessor

LiveProfessor, developed by audioström, is a plugin host software for live sound applications on Windows and macOS, supporting Virtual Studio Technology (VST) and Audio Unit (AU) plugins for real-time audio processing [11].

In this study, LiveProfessor was chosen for its flexible signal routing capabilities, used to direct stereo signals to subwoofers and satellite speakers. It applied FabFilter Pro-Q3, an equalization plugin, to implement 4th-order Linkwitz–Riley filters by cascading two 2nd-order Butterworth filters, ensuring precise frequency division with minimal phase distortion–essential for consistent FR in the experimental setup.

3 Method

3.1 Equipment and measurement setup

This study examines the effects of crossover frequency on subwoofer-satellite systems in fixed listening environments, employing 4th-order Linkwitz–Riley filters. Measurements were conducted in two distinct rooms to identify consistent FR and GD patterns. Satellite speakers, KEF R3 META and Genelec 1032C, were selected for their transparent manufacturer-provided measurements. Subwoofers included KEF Kube 15 MIE for its wide low-frequency range with a 15-inch woofer, EVE Audio TS108 to represent compact 8-inch subwoofers suitable for home use, and Genelec 7370A as a standard studio-grade subwoofer.

3.1.1 Room 1

- **Size:** 4.7 m (length) × 2.7 m (width) × 2.35 m (height);
- **Subwoofers:** KEF Kube 15 MIE (Subwoofer 1), EVE Audio TS108 (Subwoofer 2);
- **Satellite Speaker:** KEF R3 META (powered by NAD C388 amplifier, Satellite Speaker Pair 1);
- **Measurement Tools:** Earthworks M30 microphone, Antelope Orion Studio Synergy Core ADC/DAC;
- **Software:** Room EQ Wizard (REW), LiveProfessor.

In Room 1, a single satellite speaker pair was used to assess crossover frequency effects in a small-room environment. The recommended listening position is typically located at 38% of the room length from the front wall, forming an equilateral triangle with the two satellite speakers at a 60-degree angle. However, to mitigate potential near-field effects from the subwoofer while also considering low-frequency room modes, the measurement microphone was positioned at 62% of the room length from the front wall (equivalently, 38% from the rear wall) instead. Measurements were conducted at five points, with the microphone offset by 0.15 m in the up, down, left, and right directions (width & height) from the central position, to capture spatial variations in the sound field. The basic microphone measurement position was aligned with the tweeter height.

The setup is depicted in Figure 1 for the length × width view and Figure 2 for the width × height view. Measurements included Satellite Speaker Pair 1 with either Subwoofer 1 or Subwoofer 2, as shown in Figures 1a, 1b, 2a, and 2b. Precise time alignment was

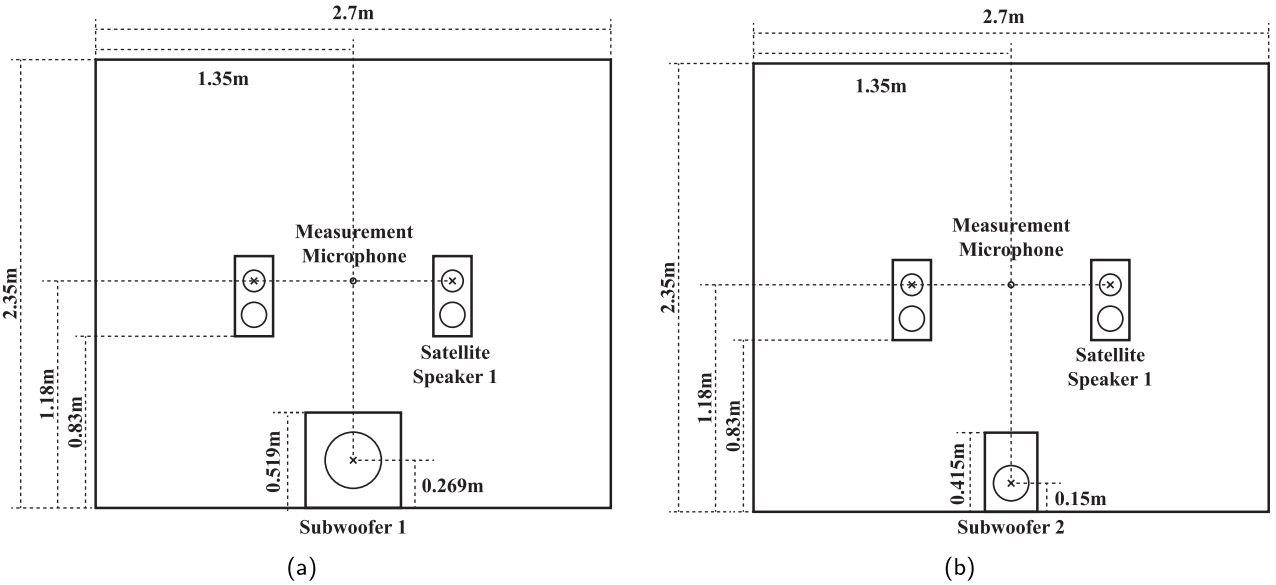

Figure 2. Measurement setups in Room 1 (width × height). (a) Subwoofer 1 and Satellite Speaker Pair 1. (b) Subwoofer 2 and Satellite Speaker Pair 1.

applied, as described in Section 3.1.4, to compensate for timing differences and ensure phase coherence.

3.1.2 Room 2

- **Size:** 6.497 m (length) × 7.96 m (width) × 2.61 m (height);
- **Subwoofer:** Genelec 7370A (Subwoofer 3);
- **Satellite Speaker:** Genelec 1032C (Satellite Speaker Pair 2);
- **Measurement Tools:** Earthworks M30 microphone, Avid Carbon ADC/DAC (with Universal Audio Volt 1 for subwoofer routing convenience);
- **Software:** Room EQ Wizard (REW), LiveProfessor.

In Room 2, located at Sangmyung University, measurements were conducted in a larger space than Room 1 to explore the impact of room size on crossover optimization. Unlike Room 1, where subwoofer placement at the corner was not feasible due to constraints from cables and room acoustic materials, Subwoofer 3 was placed at two positions to evaluate whether crossover frequency optimization remains effective in a corner placement. Measurements were conducted at two positions: Position 1 at 38% of the room length from the front wall and Position 2 at 38% of the room length from the rear wall, which is equivalently 62% from the front wall. Measurement methods, including the use of five spatially offset points and time alignment, followed the same procedure as in Room 1. The setup is depicted in Figure 3.

3.1.3 Experimental cases

The experimental cases were defined as follows:

- **Case 1:** Subwoofer 1 and Satellite Speaker Pair 1 in Room 1.
- **Case 2:** Subwoofer 2 and Satellite Speaker Pair 1 in Room 1.
- **Case 3:** Subwoofer 3 and Satellite Speaker Pair 2 in Room 2, subwoofer at the center, measured at Placement 1.
- **Case 4:** Subwoofer 3 and Satellite Speaker Pair 2 in Room 2, subwoofer at the center, measured at Placement 2.
- **Case 5:** Subwoofer 3 and Satellite Speaker Pair 2 in Room 2, subwoofer in the corner, measured at Placement 1.
- **Case 6:** Subwoofer 3 and Satellite Speaker Pair 2 in Room 2, subwoofer in the corner, measured at Placement 2.

3.1.4 Time alignment

Time delays were measured at the sample level with RTL Utility, which typically assesses internal latency via line output/input, but in this study, a measurement microphone (Earthwork m30) was connected as the input and speakers as the output to measure latency between subwoofer and satellite signals. These measurements were corrected to 0.1 ms precision in LiveProfessor to adjust temporal coherence. The measured latency values for each case, including the average latency of satellite speakers and subwoofers, as well as their differences, are summarized in Table 1.

Phase alignment was adjusted using REW measurements of the wrapped phase at 85 Hz, a frequency selected as a reference within the typical crossover range. The choice of 85 Hz aligns with the Genelec 7300 Series manual, which uses 85 Hz as the default crossover frequency for centralized bass management and recommends an 85 Hz test tone for phase alignment [12]. While a test tone was not used in this study, 85 Hz was chosen as a

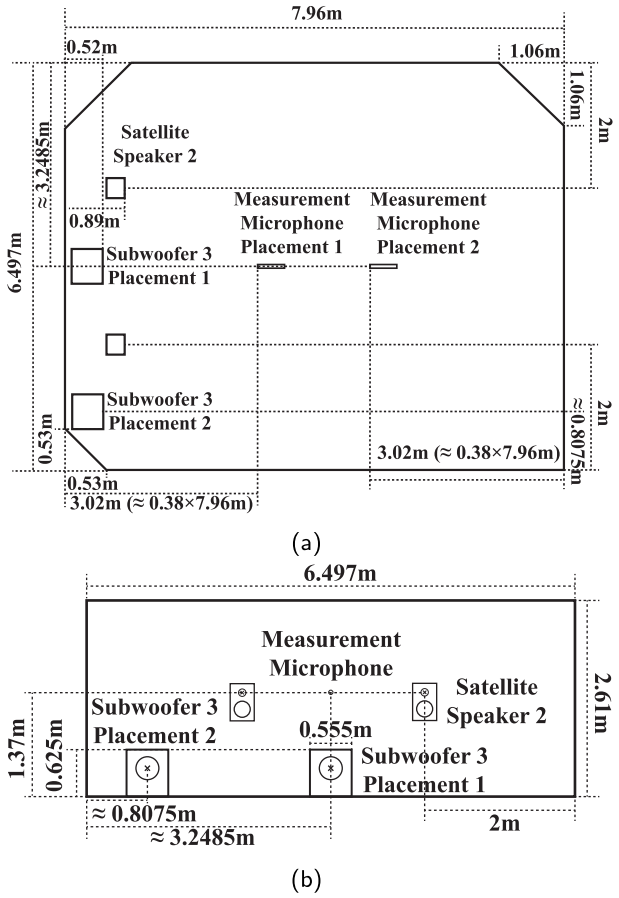

Figure 3. Measurement setups in Room 2. (a) Subwoofer 3 and Satellite Speaker Pair 2 (length × width). (b) Subwoofer 3 and Satellite Speaker Pair 2 (width × height).

Table 1. Latency measurements for time alignment.

Case	Avg Sate Latency (Samples)	Avg Sub Latency (Samples)	Latency Difference (Samples)	Latency Difference (ms)
1	1717	2093.2	376.2	7.84
2	1713	2378	665	13.85
3	4139	6095.8	1956.8	40.77
4	3878	5825.8	1947.8	40.58
5	4907	6983	2076	43.25
6	4364	6439.2	2075.2	43.23

practical reference frequency for consistency with industry standards. The wrapped phase differences between the satellite speakers and subwoofers were calculated and minimized by adjusting the subwoofer phase control settings. For Subwoofer 1 and Subwoofer 2, which support phase settings of 0 degrees or 180 degrees, the phase was set to the value closest to the measured absolute phase difference. For Subwoofer 3, which allows phase adjustments in 90-degree increments, the phase was set accordingly. The phase measurements and resulting absolute differences for each case are based on the first of three

Table 2. Wrapped phase measurements at 85 Hz for phase alignment.

Case	Satellite Speaker Phase (deg)	Subwoofer Speaker Phase (deg)	Phase Difference (deg)
1	−18	178	164
2	−18	−12	6
3	24	107	83
4	4	170	166
5	12	−171	177
6	−19	−151	132

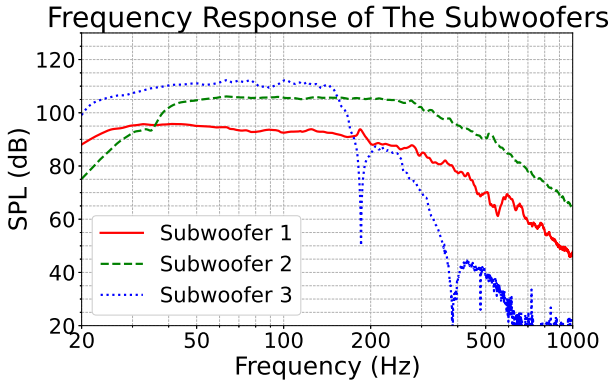

Figure 4. Frequency response measurements within 1 cm for Subwoofer 1 (KEF Kube 15 MIE), Subwoofer 2 (EVE Audio TS108), and Subwoofer 3 (Genelec 7370A) in LFE mode, with built-in low-pass filters set to maximum frequency. The plot shows a representative measurement from three repeated tests, as results were consistent across trials.

measurements per case, as the second and third measurements showed no significant variation, and are presented in Table 2. This alignment process ensures that phase-induced interference is minimized at the crossover frequency, supporting the subsequent GD minimization process detailed in Section 2.2.

3.1.5 *Volume calibration*

The SPL of the satellite speakers was initially calibrated to approximately 83 dB (C-weighted) using pink noise without the subwoofer, following the volume level suggested by Bob Katz [13]. Subsequently, with the subwoofer engaged and a crossover frequency of 140 Hz (the upper bound of the tested range) applied, the combined output was adjusted to target 83 dB (C-weighted), adhering to EBU R 128 loudness standards [14]. SPL measurements were performed using a BENETECH GM1356 microphone (35–130 dB range, 0.1 dB resolution, 2 measurements/sec). To confirm the subwoofers' response, FR measurements were conducted within 1 cm from each subwoofer in LFE mode, with their built-in low-pass filters set to the maximum frequency to reduce phase distortion. Three repeated measurements were performed, and due to their consistency, a representative measurement is shown in Figure 4, unlike the

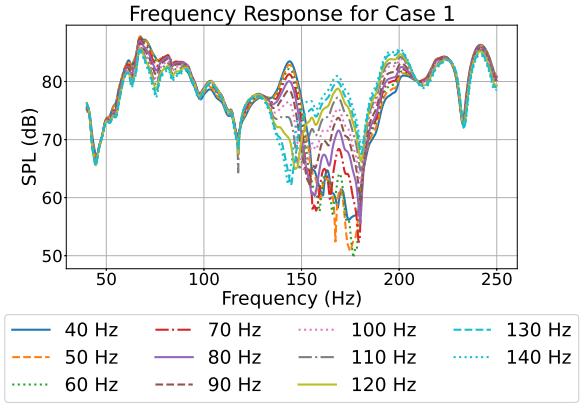

(a) Case 1: Satellite 1 + Subwoofer 1 (40–250 Hz)

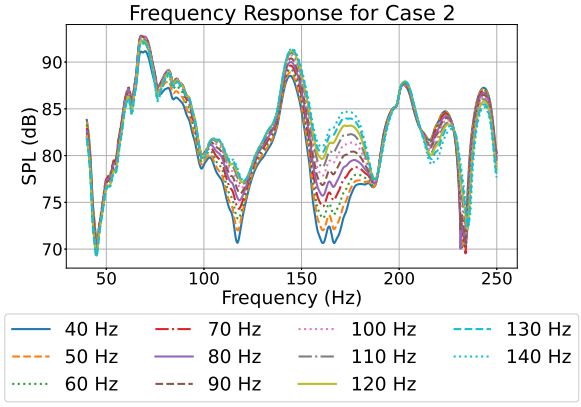

(b) Case 2: Satellite 1 + Subwoofer 2 (40–250 Hz)

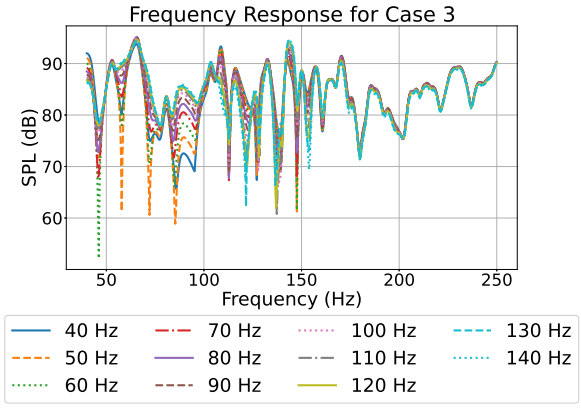

(c) Case 3: Satellite 2 + Subwoofer 1 (40–250 Hz)

Figure 5. Frequency response for Cases 1–3. (a) Case 1: Satellite 1 + Subwoofer 1 (40–250 Hz). (b) Case 2: Satellite 1 + Subwoofer 2 (40–250 Hz). (c) Case 3: Satellite 2 + Subwoofer 1 (40–250 Hz).

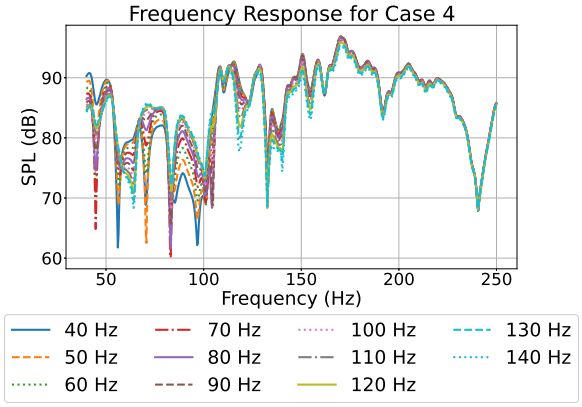

(a) Case 4: Satellite 2 + Subwoofer 2 (40–250 Hz)

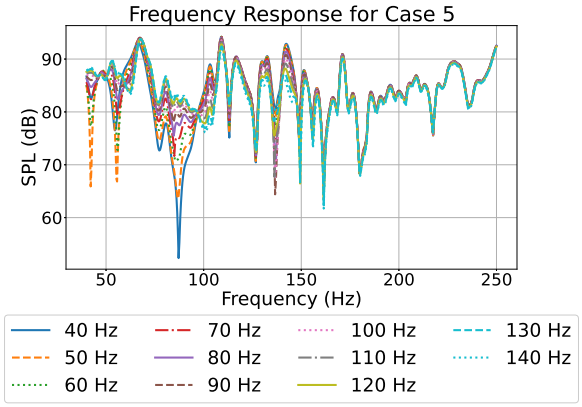

(b) Case 5: Satellite 3 + Subwoofer 3 (40–250 Hz)

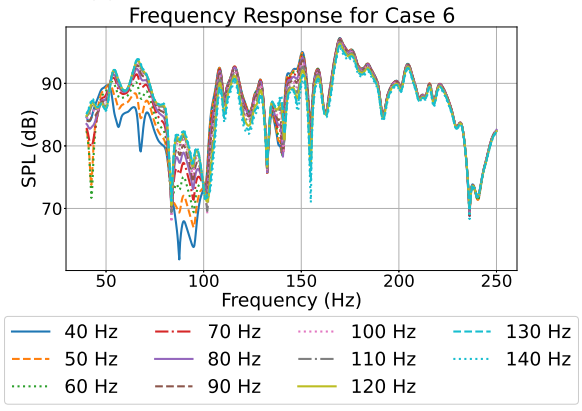

(c) Case 6: Satellite 3 + Subwoofer 4 (40–250 Hz)

Figure 6. Frequency response for Cases 4–6. (a) Case 4: Satellite 2 + Subwoofer 2 (40–250 Hz). (b) Case 5: Satellite 3 + Subwoofer 3 (40–250 Hz). (c) Case 6: Satellite 3 + Subwoofer 4 (40–250 Hz).

averaged frequency response graphs (Figs. 5a–6c) which combine multiple spatial and trial measurements. Once set, the volume controls remained fixed, and only the crossover frequency was adjusted for subsequent tests.

Spinorama graphs for the satellite speakers are provided by the manufacturers. For Satellite Speaker 1 pair, the graph is included in the KEF R Meta White Paper [15]. For Satellite Speaker 2 pair, the graph is available in the Genelec 1032C Operating Manual [16]. These graphs suggest that, within the frequency range of interest, sound pressure levels exhibit a subtle, consistent, and continuous decrease in the lower frequencies, rather than irregular variations.

3.1.6 Crossover filtering

As detailed in Section 2.2.2, 4th-order Linkwitz–Riley filters were applied to subwoofers and satellite speakers using FabFilter Pro-Q3 in LiveProfessor, cascading

two 2nd-order Butterworth filters. Crossover frequencies ranged from 40 Hz to 140 Hz in 10 Hz steps, selected via grid search to systematically assess GD and FR variations across this range.

3.2 Quantitative objective function

The optimal crossover frequency, ω_{oc}, was determined by minimizing GD, as expressed in the following equation:

$$\omega_{oc} = \arg\min_{\omega} \left(\max_{\omega_{LC}+\alpha \le \omega_i \le \omega_{HC}+\beta} |\mathrm{GD}(\omega_i)| \right) \quad (5)$$

where:

- ω_{oc}: Optimal crossover frequency;
- ω_{LC}, ω_{HC}: Minimum and maximum crossover frequency bounds;
- α, β: Adjustment factors to extend the analysis range beyond the crossover frequencies, capturing significant $\max|\mathrm{GD}|$ variations observed during experiments (detailed in Sect. 3.4);
- $\mathrm{GD}(\omega_i)$: GD at frequency ω_i.

Furthermore, by representing $\phi(\omega)$ as the phase response of the FR $H(\omega)$, it can also be formulated as:

$$\omega_{oc} = \arg\min_{\omega} \left(\max_{\omega_{LC}+\alpha \le \omega_i \le \omega_{HC}+\beta} \left| -\frac{\mathrm{d}}{\mathrm{d}\omega_i} \arg(H(\omega_i)) \right| \right) \quad (6)$$

where $H(\omega) = |H(\omega)|e^{j\phi(\omega)}$ combines magnitude $|H(\omega)|$ and phase $\phi(\omega)$. This method aims to minimize $\max|\mathrm{GD}|$ and to reduce phase-induced FR irregularities, assuming precise time alignment as detailed in Section 3.1.4. The GD Minimization Effectiveness Score ($E_{\mathrm{GD,Max}}$) quantifies the reduction in $\max|\mathrm{GD}|$ from a baseline to the optimized crossover frequency:

$$E_{\mathrm{GD,Max}}(\omega_c) = \frac{\max|\mathrm{GD}|_{\mathrm{ref}} - \max|\mathrm{GD}|_{\mathrm{opt}}}{\max|\mathrm{GD}|_{\mathrm{ref}}} \times 100\,(\%) \quad (7)$$

where:

- $\max|\mathrm{GD}|_{\mathrm{ref}}$: The maximum absolute GD at the baseline crossover frequency;
- $\max|\mathrm{GD}|_{\mathrm{opt}}$: The maximum absolute GD at the ω_c.

The baseline was set to 40 Hz, a common LFE crossover frequency often adopted in consumer audio systems. $E_{\mathrm{GD,Max}}$ measures the percentage decrease in peak GD, with higher values indicating greater GD reduction.

3.3 Evaluation metrics for frequency response consistency

To evaluate the impact of GD on FR consistency, the GD-SPL difference ($\Delta_{\text{GD-SPL}}$) was calculated for each measurement across all experimental cases. For each case, 33 measurements were collected at the basic position (3 trials × 11 crossover frequencies, ranging from 40 Hz to 140 Hz in 10 Hz steps). The $\Delta_{\text{GD-SPL}}$ quantifies the SPL reduction at the frequency where the $\max|\mathrm{GD}|$ occurs, relative to the average SPL across a specified frequency range, and is defined as:

$$\Delta_{\text{GD-SPL}}(\omega_c) = \mathrm{SPL}_{\mathrm{avg}}(\omega_c) - |H(\omega_{\mathrm{GD}})| \quad (8)$$

where:

- ω_{GD}: Frequency where $\max|\mathrm{GD}|$ occurs.
- $\mathrm{SPL}_{\mathrm{avg}}(\omega_c)$: Average SPL over the range $\omega_{LC}+\alpha$ to $\omega_{HC}+\beta$, calculated as:

$$\mathrm{SPL}_{\mathrm{avg}}(\omega_c) = \frac{1}{N}\sum_{k=1}^{N} \mathrm{SPL}(\omega_k)$$

  where N is the number of interpolation points, and ω_k are frequencies within the specified range.
- $|H(\omega_{\mathrm{GD}})|$: SPL at ω_{GD} in dB.

To assess the causal relationship between $\max|\mathrm{GD}|$ and $\Delta_{\text{GD-SPL}}$, a Fixed Effects (FE) model was applied to a panel dataset of 198 observations (6 cases × 33 measurements per case). The FE model controls for unobserved case-specific heterogeneity and is specified as:

$$\Delta_{\text{GD-SPL},i,t} = \beta_0 + \beta_1 \cdot \max|\mathrm{GD}|_{i,t} + \alpha_i + \epsilon_{i,t} \quad (9)$$

where:

- i: Case index (1 to 6).
- t: Measurement index (1 to 33 per case).
- $\Delta_{\text{GD-SPL},i,t}$: GD-SPL difference for case i at measurement t.
- $\max|\mathrm{GD}|_{i,t}$: Maximum absolute GD for case i at measurement t.
- β_0: Intercept.
- β_1: Coefficient of $\max|\mathrm{GD}|$, representing its causal effect on $\Delta_{\text{GD-SPL}}$.
- α_i: Case-specific fixed effect.
- $\epsilon_{i,t}$: Error term.

The model was estimated using clustered standard errors to account for potential within-case correlation, focusing on within-case variations to evaluate whether minimizing $\max|\mathrm{GD}|$ reduces FR irregularities. The estimation results are presented in Section 4.3.

3.4 Export data

GD values were derived by decoding base64-encoded data from REW measurements using Python, with the unique identifier (UUID) extracted to access the data. For Cases 1 and 2, the analysis range for equations (5) and (6) was set with $\alpha = 0, \beta = 110$, spanning 40–250 Hz, to capture significant $\max|\mathrm{GD}|$ variations beyond the maximum crossover frequency of 140 Hz, as substantial GD peaks were observed at 233–235 Hz (Tabs. 3 and 4 in Sect. 4.1). For Cases 3–6, as shown in Section 4.2, the frequency response (FR) graphs above 170 Hz exhibited minimal changes with variations in crossover frequency, leading to the adoption of $\alpha = 0, \beta = 30$, corresponding

Table 3. Maximum absolute value of GD (s) for different crossover frequencies (Case 1: Satellite 1 + Subwoofer 1).

Crossover Freq. (Hz)	Freq. at Max GD (Hz)	Max GD (s)	GD Std. Dev. (s)
40	168.401	0.161438	0.0174
50	167.48	0.483999	0.0396
60	175.385	0.556388	0.1337
70	155.708	0.443476	0.0056
80	180.092	0.257753	0.0051
90	152.426	0.171449	0.0090
100	150.609	0.141719	0.0019
110	148.806	0.139784	0.0013
120	147.003	0.137182	0.0009
130	145.174	0.156455	0.0024
140	233.32	0.128911	0.0003

to a 40–170 Hz range, to focus the analysis on the region with significant GD and FR variations.

As noted in Section 2.2.1, measurements had a frequency step of approximately 0.37 Hz. Cubic interpolation was applied to smooth rapid FR and GD changes, dividing the 40–250 Hz range into 210 000 points (in Cases 3–6, 40–170 Hz range into 130 000 points).

The Python project for GD data export is available at Zenodo [17]. FR data, including SPL (dB) at 0.37 Hz intervals, were extracted as text files via the REW API and interpolated to 1000 points per Hz for graphing in Python.

Raw measurement data and average FRs, including subwoofer proximity measurements, are available in [18].

3.5 Limitations

This approach conducted measurements in two rooms, which may not capture the full range of acoustic conditions present in rooms of varying sizes, shapes, or materials. The choice of specific subwoofer and satellite speaker models may limit the applicability of these findings to other equipment configurations. Likewise, the crossover frequency range of 40–140 Hz was explored. While this broad range, extending up to 140 Hz, was chosen to provide sufficient experimental data points across varied conditions for robust statistical analysis and method validation, it is important to note that crossover frequencies at the upper end of this range are generally not recommended for practical subwoofer-satellite system setup. This is primarily due to the potential for audibility of the subwoofer's location at higher frequencies, as indicated by perceptual studies [3, 4]. Thus comparisons with Bharitkar et al.'s method [5] were conducted up to 120 Hz in Section 5. The dependence on precise time alignment (Sect. 3.1.4) may not be feasible in systems with less consistent alignment accuracy.

Additionally, this study did not define a universal threshold for acceptable GD or SPL dip size, as their perceptual impact remains uncertain (Sect. 5). Measurements were conducted at fixed positions (Sect. 3.1), optimized within ±0.15 m, and larger deviations may reduce optimization effectiveness.

Table 4. Maximum absolute value of GD (s) for different crossover frequencies (Case 2: Satellite 1 + Subwoofer 2).

Crossover Freq. (Hz)	Freq. at Max GD (Hz)	Max GD (s)	GD Std. Dev. (s)
40	233.068	0.316046	0.0006
50	233.209	0.377154	0.0064
60	233.291	0.339174	0.0016
70	233.379	0.298072	0.0014
80	233.492	0.266223	0.0021
90	233.868	0.246304	0.0006
100	233.953	0.215239	0.0009
110	234.267	0.205774	0.0008
120	234.537	0.194066	0.0007
130	234.831	0.190883	0.0041
140	235.053	0.186856	0.0009

Table 5. Maximum absolute value of GD (s) for different crossover frequencies (Case 3: Satellite 2 + Subwoofer 3).

Crossover Freq. (Hz)	Freq. at Max GD (Hz)	Max GD (s)	GD Std. Dev. (s)
40	127.039	0.697627	0.0017
50	58.083	1.067816	0.0051
60	127.256	0.968843	0.0013
70	112.975	0.725834	0.0026
80	113.01	0.948499	0.0145
90	127.736	0.698518	0.0004
100	127.986	0.709892	0.0010
110	128.032	0.535337	0.0019
120	136.794	0.792829	0.0031
130	136.663	0.428247	0.0020
140	121.394	0.776674	0.0087

4 Results and analysis

The experimental conditions for Cases 1–6 are detailed in Section 3.1. Measurements were conducted three times per case, with standard deviations in Tables 3–8 representing the sample standard deviation of the three raw max |GD| measurements at each crossover frequency. FR graphs (Figs. 5a–6c) represent the average of 15 measurements per crossover frequency, comprising three repeated trials and five spatially offset positions, to ensure robust representation of the sound field.

4.1 GD minimization results

Detailed max |GD| values across crossover frequencies are provided in Tables 3–8. Few cases exhibit notable variability in max |GD| or the frequency at which it occurs, as indicated by the standard deviations. For instance, in Case 1 at 60 Hz, a high standard deviation (0.1337) was observed due to variability in the measured max |GD| values across trials, with one measurement yielding a

Table 6. Maximum absolute value of GD (s) for different crossover frequencies (Case 4: Satellite 2 + Subwoofer 3).

Crossover Freq. (Hz)	Freq. at Max GD (Hz)	Max GD (s)	GD Std. Dev. (s)
40	132.75	0.725282	0.0015
50	132.752	0.694872	0.0010
60	132.756	0.653750	0.0015
70	132.753	0.630789	0.0049
80	132.748	0.548151	0.0018
90	132.755	0.516256	0.0097
100	132.752	0.458204	0.0131
110	132.742	0.390124	0.0059
120	132.717	0.337217	0.0011
130	132.698	0.287185	0.0012
140	132.701	0.241211	0.0009

Table 7. Maximum absolute value of GD (s) for different crossover frequencies (Case 5: Satellite 2 + Subwoofer 3).

Crossover Freq. (Hz)	Freq. at Max GD (Hz)	Max GD (s)	GD Std. Dev. (s)
40	87.307	0.672502	0.0120
50	42.308	0.959056	0.0067
60	148.955	0.536077	0.0014
70	149.003	0.555531	0.0015
80	149.066	0.583029	0.0019
90	149.14	0.631075	0.0017
100	149.211	0.713622	0.0026
110	149.24	0.813086	0.0017
120	149.233	0.703154	0.0065
130	161.633	0.688304	0.0032
140	161.647	0.751619	0.0057

noticeably higher value than others, despite consistent frequencies with maximum GD around 167–175 Hz. This variability likely results from phase cancellation instabilities at this frequency. Cases 1–5 show optimal crossover frequencies (ω_{oc}) ranging from 60 Hz to 140 Hz, with $E_{GD,Max}$ ranging from 20.2% to 66.7%, as summarized in Table 9. In contrast, Case 6 yields $\omega_{oc} = 40$ Hz and $E_{GD,Max} = 0.0\%$, as 40 Hz serves as the baseline frequency.

4.2 FR analysis

Figures 5a–6c show FR variations across all tested crossover frequencies. In Cases 1–5, minimizing max |GD| at optimal crossover frequencies (60–140 Hz) reduces SPL dips, as observed in the graphs. This reduction is quantitatively validated in Section 4.3. In Case 6, where max |GD| is minimized at 40 Hz, larger SPL dips appear at higher crossover frequencies, indicating a distinct optimal crossover response compared to Cases 1–5.

Table 8. Maximum absolute value of GD (s) for different crossover frequencies (Case 6: Satellite 2 + Subwoofer 3).

Crossover Freq. (Hz)	Freq. at Max GD (Hz)	Max GD (s)	GD Std. Dev. (s)
40	133.078	0.193026	0.0021
50	42.463	0.269523	0.0028
60	42.559	0.240810	0.0039
70	83.504	0.284278	0.0001
80	83.501	0.410191	0.0009
90	83.522	0.563704	0.0073
100	83.613	0.723909	0.0080
110	83.598	0.624583	0.0046
120	83.574	0.535636	0.0038
130	83.577	0.479987	0.0019
140	154.908	0.452185	0.0014

Table 9. Summary of optimal crossover frequencies, maximum absolute value of GD, and $E_{GD,Max}$ across cases.

Case	Crossover Freq. (Hz)	Max Abs. GD (s)	Freq. at Max GD (Hz)	$E_{GD,Max}$ (%)
1	140	0.128911	233.32	20.2
2	140	0.186856	235.053	40.9
3	130	0.428247	136.663	38.6
4	140	0.241211	132.701	66.7
5	60	0.536077	148.955	20.3
6	40	0.193026	133.078	0.0

4.3 Statistical and comparative insights

The FE model results, estimating the causal relationship between max |GD| and $\Delta_{GD\text{-}SPL}$, are summarized in Table 10. The model reveals a statistically significant effect of max |GD| on $\Delta_{GD\text{-}SPL}$, with a coefficient of 22.274 (p-value < 0.0001). This indicates that a 1-unit increase in max |GD| leads to an average increase of 22.274 dB in $\Delta_{GD\text{-}SPL}$, with a 95% confidence interval of [15.760, 28.787]. The R-squared (Within) value of 0.2633 shows that max |GD| explains approximately 26.33% of the within-case variation in $\Delta_{GD\text{-}SPL}$. This R-squared value suggests that the variability in $\Delta_{GD\text{-}SPL}$ is influenced by a range of complex and interrelated acoustic factors, such as room modes, reflections, or non-minimum phase characteristics, which are inherent to real-world listening environments. Despite the contribution of these factors, the F-test for poolability ($F = 16.617$, p-value < 0.0001) confirms significant differences across cases, supporting the use of the FE model.

Table 11 provides descriptive statistics of max |GD| and $\Delta_{GD\text{-}SPL}$ at specific crossover frequencies for each case. The table reports the maximum and minimum max |GD| values across the 33 measurements per case, along with the corresponding $\Delta_{GD\text{-}SPL}$ values and crossover frequencies (ω_c). For Cases 1–5, minimizing

Table 10. Fixed effects model results for the effect of max |GD| on $\Delta_{\text{GD-SPL}}$.

Parameter	Estimate	Std. Err.	T-stat	P-value	95% CI
Const	11.663	1.5311	7.6174	<0.0001	[8.6428, 14.683]
max|GD|	22.274	3.3021	6.7453	<0.0001	[15.760, 28.787]
R-squared (Within): 0.2633					
F-test for Poolability: 16.617 (p-value < 0.0001)					

Table 11. Maximum and minimum max |GD| and corresponding $\Delta_{\text{GD-SPL}}$ across cases.

	Max GD		Min GD	
Case	ω_c (Hz)	$\Delta_{\text{GD-SPL}}$ (dB)	ω_c (Hz)	$\Delta_{\text{GD-SPL}}$ (dB)
1	60	44.38	140	9.69
2	50	21.62	130	15.02
3	50	20.02	80	18.69
4	40	21.86	140	18.04
5	50	20.75	60	15.59
6	100	35.59	40	11.41

max |GD| reduces $\Delta_{\text{GD-SPL}}$ from 20.02–44.38 dB to 9.69–18.69 dB. In Case 6, $\Delta_{\text{GD-SPL}}$ decreases from 35.59 dB at 100 Hz to 11.41 dB at 40 Hz, a 24.18 dB improvement.

To explore practical applicability within a perceptually more constrained range, the optimal crossover frequencies within 40–120 Hz were additionally analyzed (Tab. 12). This range was chosen, in part, based on perceptual studies suggesting subwoofer localization might become discernible above 85–120 Hz [3, 4]. Table 12 appears to indicate that the GD minimization approach tends to remain effective in this range, potentially showing reductions in max |GD| and $\Delta_{\text{GD-SPL}}$, suggesting its possible relevance for studio and home audio applications.

These findings confirm that minimizing max |GD| effectively reduces FR irregularities, as evidenced by the significant causal effect in the FE model and the consistent patterns observed in the descriptive statistics.

5 Discussion

Minimizing max |GD| appears to offer a potential approach for reducing GD and FR irregularities in subwoofer-satellite systems, possibly improving time-domain accuracy for applications such as studio monitoring and home audio. Across Cases 1–6, this method seems associated with lower $\Delta_{\text{GD-SPL}}$ and reduced SPL dips, as suggested by statistical findings in Section 4.3 and visually indicated by Figures 5a–6c. The experimental range of 40–140 Hz provided data exploring the method's applicability across various crossover frequencies.

While the method generally shows association with reduced $\Delta_{\text{GD-SPL}}$ across cases, Case 6 presents a distinct result. In Case 6, with max |GD| minimized at the 40 Hz baseline (Eq. (7)), an $E_{\text{GD,Max}}$ of 0.0% was observed, unlike Cases 1–5 (Tab. 9). This indicates that 40 Hz was the optimal frequency for minimizing max |GD| in this specific setup. The $\Delta_{\text{GD-SPL}}$ at 40 Hz was 11.41 dB, which is significantly lower than the 35.59 dB observed at 100 Hz (Tab. 12), a frequency associated with a higher max |GD| in this case. This suggests that in certain conditions, the baseline frequency may already represent the minimum max |GD| point within the tested range.

Table 12. Optimal crossover frequencies, maximum absolute value of GD, $E_{\text{GD,Max}}$, and $\Delta_{\text{GD-SPL}}$ in the 40–120 Hz range across cases.

Case	Crossover Freq. (Hz)	Max Abs. GD (s)	Freq. at Max GD (Hz)	$E_{\text{GD,Max}}$ (%)	$\Delta_{\text{GD-SPL}}$ (dB)
1	120	0.137182	147.003	15.0	16.40
2	120	0.194066	234.537	38.6	15.43
3	110	0.535337	128.032	23.3	18.57
4	120	0.337217	132.717	53.5	19.48
5	60	0.536077	148.955	20.3	15.59
6	40	0.193026	133.078	0.0	11.41

Table 13. Optimal crossover frequencies and minimum spectral deviations using Bharitkar et al. method (40–120 Hz).

Case	ω_{oc} (Hz)	Min Spectral Deviation
1	120	5.375
2	120	4.912
3	90	5.975
4	120	6.379
5	120	5.171
6	120	5.552

To compare with prior methods, the spectral deviation metric from Bharitkar et al. [5] was applied to interpolated FR data (in Cases 1–2, 40–250 Hz, in Cases 3–6, 40–170 Hz, 0.001 Hz spacing), constrained to the crossover frequency practical range of 40–120 Hz. Table 13 presents the optimal crossover frequencies (ω_{oc}) and minimum spectral deviations (σ_H) for this comparison, where lower σ_H may suggest improved FR flatness. Comparison shows the Bharitkar method aligns with max |GD| minimization in Cases 1, 2, and 4 (all selecting 120 Hz within this range), but may differ in Cases 3 (90 Hz for Bharitkar vs. 110 Hz for max |GD|), 5 (120 Hz for Bharitker vs. 60 Hz for max |GD|) and 6 (120 Hz for Bharitkar vs. 40 Hz for max |GD|). These differences suggest that while the Bharitkar method prioritizes FR flatness (σ_H) it may not fully address phase-related distortions, which are more directly targeted by minimizing (max |GD|). This aligns with the observed $\Delta_{\text{GD-SPL}}$ trends for the respective optimal frequencies (Tab. 11).

The statistical analysis in Section 4.3 highlights that the FE model's relatively low R-squared (0.2633) indicates that max |GD| explains only a portion of the variation in $\Delta_{\text{GD-SPL}}$, suggesting that environmental factors like room modes and reflections play a significant role.

This is particularly evident in Cases 3 and 5, conducted in Room 2, where pronounced low-frequency comb filtering is observed in Figures 5c and 6b. This comb filtering is likely caused by interference from reflected waves off Room 2's reflective surfaces, such as marble or concrete flooring, which create rapid phase shifts and amplitude dips in the FR. These effects are more noticeable at closer listening positions (Case 3 and 5) compared to Cases 4 and 6.

To further explore the impact of room acoustics, FR irregularities were analyzed in relation to room modes. In Cases 1 and 2, conducted in Room 1 (1.7 m × 2.7 m × 2.35 m), notable SPL dips are observed around 116 Hz and 233 Hz in Figures 5a and 5b. These dips likely result from room modes, calculated based on Room 1's dimensions. Specifically, the 233 Hz region corresponds to multiple higher-order modes, including tangential modes (0–2–3, 0–6–1, 0–5–2 at 230.78–233.65 Hz) and oblique modes (1–1–3, 3–3–1, 2–5–1 at 230.87–233.99 Hz), as derived from the room mode equation $f = \frac{c}{2}\sqrt{\left(\frac{n_x}{L}\right)^2 + \left(\frac{n_y}{W}\right)^2 + \left(\frac{n_z}{H}\right)^2}$, where c is the speed of sound (340 m/s), and L, W, H are the room dimensions. These modes overlap near 233 Hz, amplifying phase cancellations and resulting in prominent FR dips. Notably, the 116 Hz dip varies with changes in crossover frequency (ω_c), reflecting crossover-related phase interactions, whereas the 233 Hz dip remains consistent across ω_c, indicating its dominance by room modes. As this frequency range lies above the subwoofer's primary operating region (40–140 Hz), the observed irregularities are predominantly driven by room characteristics rather than crossover effects.

Similarly, in Room 2 (6.497 m × 7.96 m × 2.61 m), Cases 3 and 5 (measured at Position 1, 3.02 m from the front wall) and Cases 4 and 6 (measured at Position 2, 3.02 m from the rear wall) exhibit comparable FR patterns above approximately 170 Hz, as shown in Figures 5c, 6b, 6a, and 6c.

GD minimization appears beneficial but may not fully mitigate FR irregularities caused by environmental factors, particularly above the subwoofer's primary range. To mitigate such influences, this phase-centric approach might be combined with physical acoustic treatments, room construction improvements, or optimized speaker and listening position placement. For instance, integrating acoustic materials, such as melamine foams with optimized pore size polydispersity for low-frequency absorption [19], or edge absorbers designed to reduce low-frequency reverberation [20], could enhance the effectiveness of GD minimization by mitigating room modes and comb filtering observed in Cases 3 and 5. Such combined strategies may lead to more consistent FR and improved audio quality in practical settings.

For practical deployment, particularly in applications like studio monitoring and home audio, prioritizing crossover frequencies within the perceptually relevant range of 40–120 Hz might be advisable. This range is typically constrained to help prevent subwoofer localization, aligning with perceptual studies [3, 4]. Table 12 summarizes the optimal crossover frequencies and max |GD| reductions specifically within this range, suggesting the potential applicability and benefits of the GD minimization approach even when limited to perceptually appropriate settings.

Future studies could explore this method in diverse acoustic setups, potentially refining crossover optimization for specific environments. Research by Liski et al. [21, 22] indicates that GD variations above 300 Hz are perceptible (thresholds ∼0.64 ms), but the perceptual impact of low-frequency GD below 120 Hz remains an area for further investigation. Controlled listening tests, possibly incorporating varied room acoustics, could help clarify its effect on perceived audio quality and the overall impact of GD minimization in practical scenarios.

6 Conclusion

This study suggests that minimizing max |GD| may offer a phase-centric approach to potentially reducing FR irregularities in subwoofer-satellite systems. Across various experimental setups, this method appears to support improved low-frequency consistency, as explored in Section 5.

For practical applications such as studio monitoring or home audio, selecting crossover frequencies within the perceptually relevant 40–120 Hz range may help minimize subwoofer localization issues [3, 4]. To minimize room mode effects, listening positions in this study were set at 38% and 62% of the room length from the front wall (within ±0.15 m), but the effectiveness of this approach in other positions, such as those where near-field effects occur due to proximity to the subwoofer, remains uncertain. The presence of environmental factors like room modes and reflections suggests that combining this method with physical acoustic treatments or optimized speaker placement could further enhance flatter FR. Crossover frequencies above 120 Hz might be considered less suitable for practical use due to potential localization issues. Future studies could explore this method's effectiveness at non-optimal listening positions, such as near-field or off-axis locations.

The GD-based approach appears applicable across the tested room and speaker setups, providing a systematic method for crossover optimization focused on phase effects. This method could potentially offer engineers a practical tool to enhance low-frequency reproduction in studio environments and is likely relevant for consumer home audio systems utilizing subwoofers.

Funding

This research received no specific grant from any funding agency in the public, commercial, or not-for-profit sectors.

Conflicts of interest

The author declares no conflict of interest.

Data availability statement

The Python code for data analysis is available in Zenodo, under the reference [17]. The research data associated with this article are available in Zenodo, under the reference [18].

References

1. M. Oehler, C. Reuter, I. Czedik-Eysenberg: Dynamics and low-frequency ratio in popular music recordings since 1965, in: Audio Engineering Society Conference: 57th International Conference: The Future of Audio Entertainment TechnologyCinema, Television and the Internet. Audio Engineering Society, Hollywood, CA, USA, 2015, pp. 1–8.
2. K.R. Holland: The Yamaha NS10M: twenty years a reference monitor. Why? Institute of Acoustics 23 (2001) 29–38.
3. N. Zacharov, S. Bech, D. Meares: The use of subwoofers in the context of surround sound program reproduction. Journal of the Audio Engineering Society 46 (1998) 276–287.
4. A. Kelloniemi, J. Ahonen, O. Paajanen, V. Pulkki: Detection of subwoofer depending on crossover frequency and spatial angle between subwoofer and main speaker, in: Proceedings of 118th Convention of the Audio Engineering Society. Barcelona, Spain, 2005, paper 6431.
5. S. Bharitkar, C. Kyriakakis: Automatic crossover frequency selection for multichannel home-theater applications, in: Proceedings of IEEE International Conference on Multimedia and Expo (ICME), Amsterdam, The Netherlands, 2005, pp. 1–4.
6. R. Miller III: Physiological and content considerations for a second low-frequency channel for bass management, subwoofers, and LFE, in: Proceedings of 118th Convention of the Audio Engineering Society, Barcelona, Spain, 2005, paper 6628.
7. W.L. Martens: The impact of decorrelated low-frequency reproduction on auditory spatial imagery: Are two subwoofers better than one? in: Proceeding of 16th International Conference on Audio Engineering Society, Spatial Sound Reproduction, Rovaniemi, Finland, 1999, paper 16-006.
8. S. Butterworth: On the theory of filter amplifiers. Wireless Engineer 7 (1930) 536–541.
9. S.H. Linkwitz: Active crossover networks for noncoincident drivers. Journal of the Audio Engineering Society 24 (1976) 2–8.
10. R.C. Heyser: Loudspeaker phase characteristics and time delay distortion: Part 1. Journal of the Audio Engineering Society 17 (1969) 30–41.
11. Audioström: LiveProfessor: live-oriented plugin host for audio processing, https://audiostrom.com/liveprofessor, accessed: February 25, 2025.
12. Genelec: Operating manual 7300 series Genelec 7360A and 7370A smart active subwoofers, https://assets.ctfassets.net/4zjnzn055a4v/2xfj0AkjCUMkM4msUE0Aiw/abf7c0a2fe9860608d89b063fe51254c/7360_and_7370_op-man_a_0.pdf, accessed: April 17, 2025.
13. B. Katz: Mastering Audio: The Art and the Science, 3rd edn. Focal Press, Oxford, 2014.
14. European Broadcasting Union: EBU R 128: Loudness normalisation and permitted maximum level of audio signals. Tech. Rep., Geneva, Switzerland, 2014, https://tech.ebu.ch/publications/r128.
15. KEF: R Meta White Paper: R Series with MAT, https://us.kef.com/pages/documents, accessed: July 9, 2025.
16. Genelec: Operating manual: Genelec 1032C, https://www.genelec.com/1032c, accessed: July 9, 2025.
17. J. Kim: A python code for exporting REW (Room EQ Wizard) group delay data [Program]. Zenodo. https://doi.org/10.5281/zenodo.15847752, 2025.
18. J. Kim: REW measurement data for the study, group delay-driven crossover optimization for subwoofer satellite system at listening position [Data set]. Zenodo. https://doi.org/10.5281/zenodo.15250615, 2025.
19. C.T. Nguyen, D. Li, Z. Xiong, M. He, L. Gautron, A. Duval, C. Perrot: Structure-property relationships of polydisperse open-cell foams: application to melamine foams. Acta Acustica 8 (2024) 42.
20. F. Kraxberger, E. Kurz, W. Weselak, G. Kubin, M. Kaltenbacher, S. Schoder: A validated finite element model for room acoustic treatments with edge absorbers. Acta Acustica 7 (2023) 44.
21. J. Liski, A. Mäkivirta, V. Välimäki: Audibility of group-delay equalization. IEEE/ACM Transactions on Audio, Speech, and Language Processing 29 (2021) 2189–2201.
22. J. Liski, A. Mäkivirta, V. Välimäki: Audibility of loudspeaker group-delay characteristics, in: Proceedings of 144th Convention on Audio Engineering Society, Milan, Italy, 2018, pp. 879–888.

Cite this article as: Kim J. 2025. Group delay-driven crossover optimization for subwoofer satellite systems at listening position. Acta Acustica, **9**, 51. https://doi.org/10.1051/aacus/2025037.